The Free Internet Journal for Organic Chemistry

Paper

Archive for Organic Chemistry

Arkivoc **2020**, part vii, 0-0

to be inserted by editorial office

Mono-*endo*-6-*N,N*-diethylcarbamoyl and Bis-*endo,endo*-6,12-*N,N*-diethylcarbamoyl derivatives of Tröger's Base. Synthesis and *exo-endo* isomerization study

Sami Dawaigher,[a] Emil Lindbäck,[a] Daniel Strand,[a] Anna Cederbalk,[a] Stuart Winikoff,*[b] Michael Harmata,*[c] Victor Snieckus,*[d] and Kenneth Wärnmark*[a]

[a] *Centre for Analysis and Synthesis, Department of Chemistry, Lund University. P. O. Box 124, 22100 Lund, Sweden*

[b] *Department of Chemistry, Truman State University, Kirksville, MO 63501, U.S.A.*

[c] *Department of Chemistry, University of Missouri, Columbia, MO 65211, U.S.A.*

[d] *Department of Chemistry, Queen's University, Kingston, ON K7L 3N6, Canada*

Email: swinikoff@truman.edu; harmatam@missouri.edu; victor.snieckus@chem.queensu.ca; kenneth.warnmark@chem.lu.se

This paper is dedicated to our mentor, colleague, and friend, Jan Bergman

Received 02-21-2020 **Accepted** 05-16-2020 **Published on line** 05-29-2020

Abstract

An efficient synthetic route to the mono-*endo*-6-*N,N*-diethylcarbamoyl and bis-*endo,endo*-6,12-*N,N*-diethylcarbamoyl derivatives of Tröger's base (TB), *endo*-**7** and *endo*-**8**, is reported. Studies of reaction time, proton source, and additive allowed establishment of optimized conditions for the conversion of *exo*-**7** into the corresponding isomer *endo*-**7**. With a longer reaction time, the *exo,exo*-6,12 bis-carbamoyl derivative *exo*-**8** was converted into the corresponding *endo,endo*-bis-carbamoyl product *endo*-**8**. Single crystal X-ray crystallographic analysis confirmed the structural and stereochemical assignments made on the basis of ^{1}H NMR, mechanistic, and computational studies. Deuterium quench experiments using LDA, CD_3ONa/CD_3OD and DCl/CD_3OD conditions of both *exo*-**7** and *exo*-**8** afforded *exo*-**7***d*$_1$ and *exo*-**8***d*$_2$, respectively (> 95% deuterium incorporation), supporting an enolate mechanism for the isomerization. In contrast, when repeating the experiment with DCl/CD_3OD, no deuterium was incorporated, suggesting the traditional ring-opening mechanism involving an iminium ion.

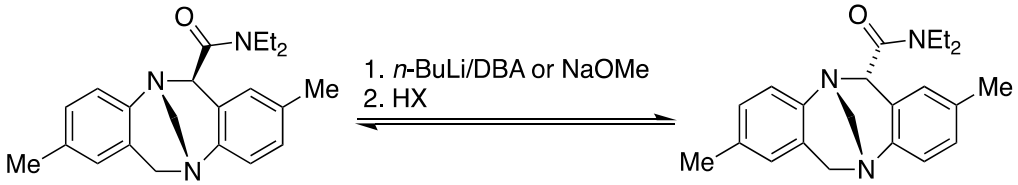

exo-**7** *endo*-**7**

Keywords: Tröger's Base, Enolates, Diastereoselectivity, Amides, Deuterium Quench

Introduction

First synthesized in 1887,[1] Tröger's base, 2,8-dimethyl-6*H*,12*H*-5,11-methanodibenzo[*b*,*f*][1,5]diazocine, (TB, **1**, (*S*,*S*) in Fig. 1), is a unique V-shaped C_2-symmetric molecule with chirality arising from pyramidal nitrogen atoms structurally incapable of undergoing inversion. Many derivatives of TB have been developed for diverse applications. These include, for example, a pH sensitive turn-on fluorescent probe,[2,3] a protein detector,[4] gas separation membranes,[5-7] CO_2 absorbents,[8-11] a dopant for liquid crystals in display screens,[12] and a chemical torsion balance.[13-17] Both TB itself and certain derivatives have elicited interest as ligands in catalysis.[18,19] Recent reviews detail the numerous possible applications of this important molecule and its congeners.[20-23]

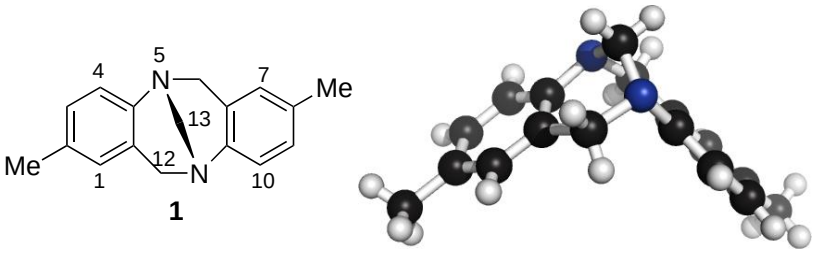

1

Figure 1. Tröger's base (**1**, TB) shown as its (*S*,*S*)-enantiomer.

Due to the versatility of **1** and its derivatives, many research groups[24] including ours,[25-30] have developed procedures to modify **1** to prepare new derivatives and analogues. Having functional groups pointing towards the inside of the chiral pocket of **1** might allow the installation of new binding sites on the concave face of TB. To date, the only method available to synthesize *endo*-functionalized derivatives of **1** has been by oxidation of one or both of the benzylic methylene groups, which results in a twisted amide or diamide, respectively.[26,31] Such amides lack the conjugation of conventional amides and are consequently more reactive, often behaving like ketones. Thus, a Wittig reaction and subsequent catalytic hydrogenation of the resulting alkenes and ester reduction selectively affords the *endo*-substituted compounds **4** and **6** shown in Scheme 1.[26] The major drawbacks of this method are the oxidation step used to prepare both monolactam **2** (10%) and dilactam **5** (28%) and the difficulties removing the phosphine oxide by-products resulting from the Wittig reaction, leading to the derivatives **4** and **6** after hydrogenation.

As part of our long-standing interest in lithiation chemistry of TB,[18,25,32-33] we considered carbanionic chemistry to functionalize one or both of the *endo* positions of TB. We have previously reported[25] on the LDA-mediated synthesis of mono-*exo*-6- and bis-*exo,exo*-6,12-*N*,*N*-dialkylcarbamoyl derivatives of TB, *exo*-**7** and *exo*-**8**, respectively (Figure 2). Herein, we disclose a comprehensive and efficient synthesis of *endo*-**7** and *endo*-**8** through an *exo,endo*-isomerization study to achieve optimization of conditions for the formation of both *exo* and *endo* isomers of the mono- and di-carbamoyl derivatives.

Thus, we report a thorough investigation of factors of temperature, time, amount and type of base and chelating additive, and type of electrophile quench for the establishment of optimized conditions to obtain preparative amounts of **7** and **8**, respectively. Additionally, we describe the reactions of a weak base (MeONa) and HCl with both proton and deuterium quench of TB and the mono-carbamoyl derivative **7**. Of interest is the fact that isomerization of TB under acidic conditions occurs, as predicted from racemization studies,[13] via methylene bridge opening-reclosure and therefore, as expected, in the case of both **1** and derivative **7**, does not lead to proton-deuterium exchange.

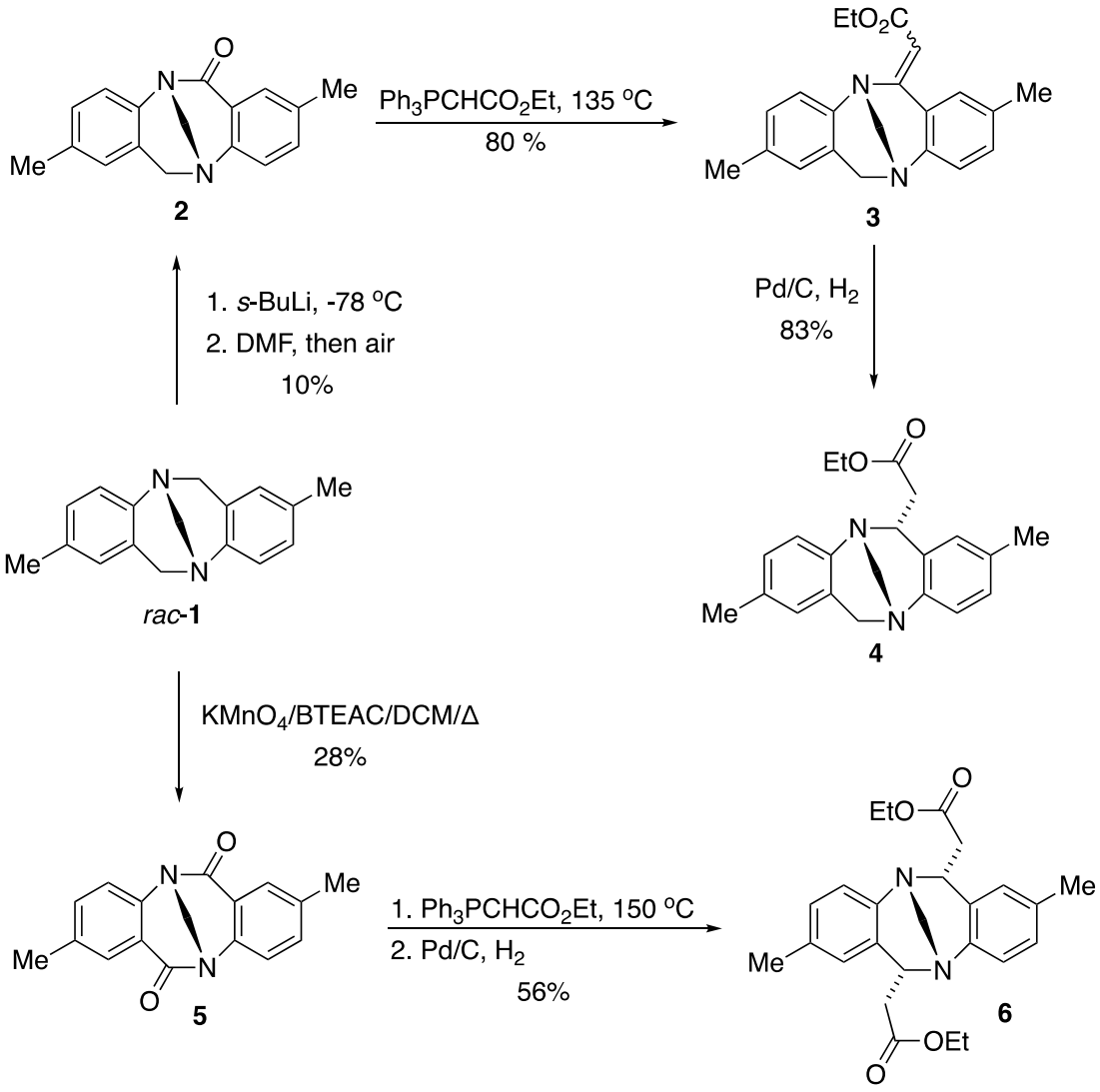

Scheme 1. Synthesis of twisted amides and TB derivatives.

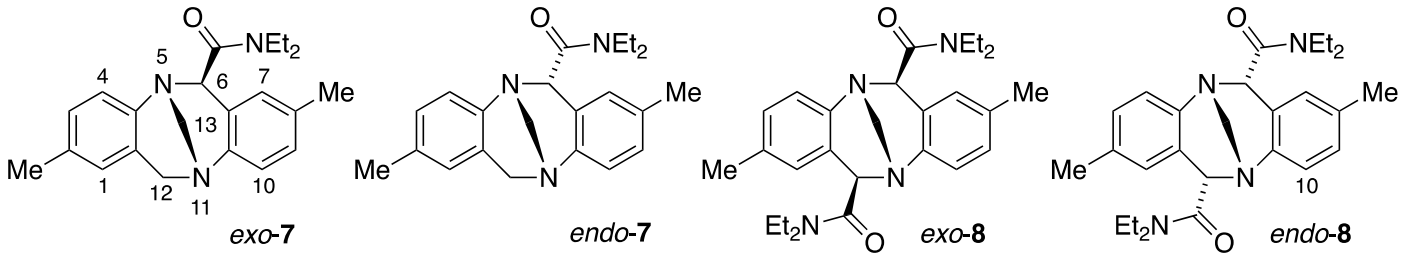

Figure 2. Derivatives of Tröger's base of the present study.

Results and Discussion

To begin, variation of the reaction temperature for *exo*-**7** to *endo*-**7** isomerization was studied and the results are displayed in Table 1. Thus, *exo*-**7** and DIPA (diisopropylamine) were combined in a minimum amount of THF and the mixture was cooled to the desired temperature. Slow dropwise addition of *n*-BuLi was followed

by stirring for 2 h and then protic quench with excess methanol. After workup, the crude product was dissolved in chloroform-*d* and the *endo*:*exo* ratio was established by comparison of the relative integrals of the peaks at δ5.40 and δ4.91 ppm in the ^{1}H NMR, which correspond to the proton alpha (H-6, Fig 2) to the carbonyl group in *endo*-**7** and *exo*-**7**, respectively. Correspondingly for *endo*-**8** and *exo*-**8**, the peaks at *δ*4.91 and *δ*4.89 ppm, were used. As seen in Table 1, the temperature that favors *endo*-**7** product formation appears to be -20 °C (entry 5). At -10 °C, on the other hand, decarbamoylated product **1** was obtained (entry 6) by a Haller-Bauer process[34] in addition to a minor ketone product resulting from *n*-BuLi addition to the amide. The structural assignments were based on the ^{1}H NMR spectra (see the Supporting Information).

Table 1. Isomerization of *exo*-**7** to *endo*-**7**. Optimization of the Reaction Temperature

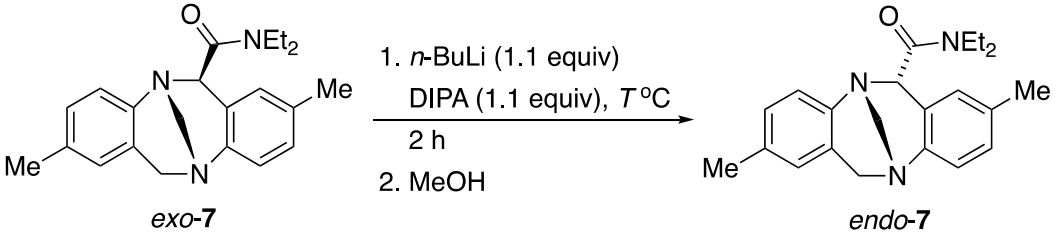

exo-**7** *endo*-**7**

Entry	T °C	*Endo*-**7**:*Exo*-**7** Ratio[a]
1	-78	0: 100
2	-50	27:73
3	-40	8:92
4	-30	2:98
5	-20	49:51
6	-10	46:54[b]

[a]Derived from ^{1}H NMR spectra of the worked-up reaction mixtures (see Experimental Section) by comparison with authentic pure materials. Reaction run until no change in composition of reaction mixture. *exo*-**7** and *endo*-**7** were the only products unless otherwise stated. [b] The ratio is based on the ^{1}H NMR spectrum of the remaining material, 90% of which is represented by **1**.

We next tested a set of selected *n*-BuLi-amine base combinations for the isomerization reaction (Table 2). Not surprisingly, at -20 °C, *n*-BuLi alone (entry 1), with TMEDA (entry 2), or with DIPEA (Hünig's base) (entry 3) afforded the decarbamoylated product **1**, the result of a Haller-Bauer reaction [34] LDA, whether generated In situ (entry 4) or as a commercial stock solution (entry 5), afforded a high ratio of *endo*-**7**:*exo*-**7**. A stock solution of LiHMDS, a weaker base (pK_a ~26 of the corresponding acid) compared to LDA (pK_a ~36 of the corresponding acid), gave a lower ratio of *endo*-**7**:*exo*-**7** (entry 6). Two other lithium dialkylamine bases generated in situ from diethylamine (DEA) and dibutylamine (DBA) were tested. The latter (LiDBA) gave the best result (compare entries 7 and 8, Table 2).

Optimization of reaction time for the formation of *endo*-**7** product was next studied (Table 3). Using the same conditions as those described for temperature optimization (Table 1) but maintaining the temperature at -20 °C, the reaction time was varied. The optimum time for the formation of *endo*-**7** was 3 h (entry 4) after

which time the product distribution remained constant (entries 4 and 5). This suggests that deprotonation is not rapid, as might be expected, since a bulky base must effect a proton abstraction on the concave face of *endo*-**7**.

Table 2. Isomerization of *exo*-**7** to *endo*-**7**. Optimization of the Base

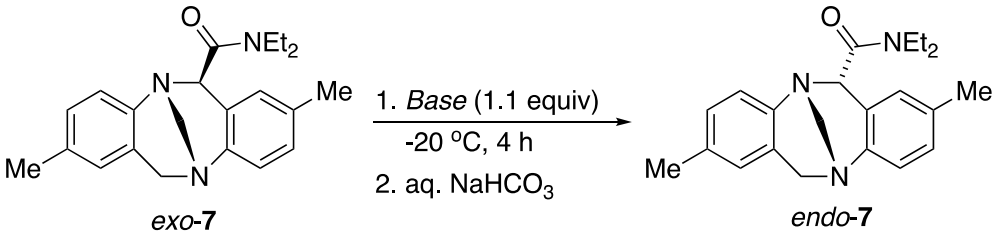

exo-**7** *endo*-**7**

Entry	Base (equiv)/Amine (equiv)	*Endo*-**7**:*Exo*-**7** Ratio[a]
1	*n*-BuLi (1.1)	0:0[b]
2	*n*-BuLi (1.1)/TMEDA (1.1)	0:0[b]
3	*n*-BuLi (1.1)/DIPEA (1.1)	0:0[b]
4	*n*-BuLi (1.1)/DIPA (1.1)	82:18
5	LDA (1.1)	82:18
6	LiHMDS (1.1)	32:68
7	*n*-BuLi (1.1)/DEA (1.1)	80:20
8	*n*-BuLi (1.1)/DBA (1.1)	86:14

[a]Derived from ^{1}H NMR spectra of the worked-up reaction mixtures (see Experimental Section) by comparison with authentic pure materials. Reaction run until no change in composition of reaction mixture. *exo*-**7** and *endo*-**7** were the only products unless otherwise stated. [b]Compound **1** was the only isolated material.

Table 3. Isomerization of *exo*-**7** to *endo*-**7**. Optimization of the Reaction Time using DIPA as Base

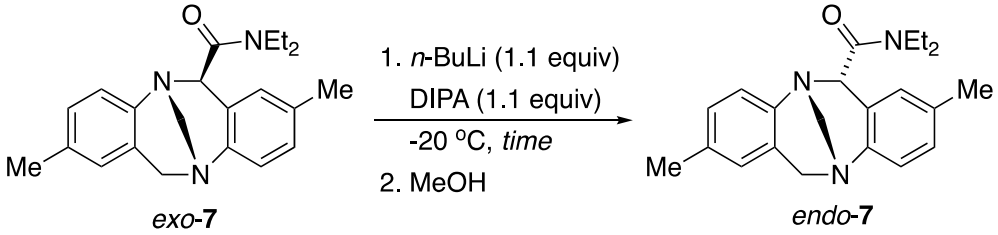

exo-**7** *endo*-**7**

Entry	Time	*Endo*-**7**:*Exo*-**7** Ratio[a]
1	1 min	2:98
2	1 h	35:65
3	2 h	49:51
4	3 h	82:18
5	6 h	82:18

[a]Derived from ^{1}H NMR spectra of the worked-up reaction mixtures (see Experimental Section) by comparison with authentic pure materials. Reaction run until no change in composition of reaction mixture. *exo*-**7** and *endo*-**7** were the only products. [b]Variation of the quenching reagent (MeOH, water, $NaHCO_3$ aq sat'd solution, and *i*-PrOH/THF showed minor variation in *endo*-**7**:*exo*-**7** ratios (79:21 – 82:18).

In view of the favorable isomerization result using LiDBA generated in situ, we tested this combination in the reaction as a function of time (Table 4). Rewardingly, the maximum *endo*-**7**:*exo*-**7** ratio was observed in shorter reaction times (entry 3) than that obtained using LDA as the base (Table 2, entry 4) and this ratio underwent essentially no variation with increasing time periods (Table 4, entries 4-6). Variation of the *n*-BuLi-DBA stoichiometry from 1.1, to 2 or 3 equivalents under the conditions given in Table 4 showed only a minor effect on the *endo*-**7**:*exo*-**7** ratio. This is not surprising, as we expect the *endo*:*exo* ratio to be determined at the acidic quench stage and the quench to be kinetic in nature. A preparative scale synthesis of *endo*-**7** from *exo*-**7** was carried out based on the optimum conditions for the isomerization, affording *endo*-**7** in 86% yield of isolated product.

Table 4. Isomerization of *exo*-**7** to *endo*-**7**. Optimization of reaction conditions using *n*-BuLi/DBA

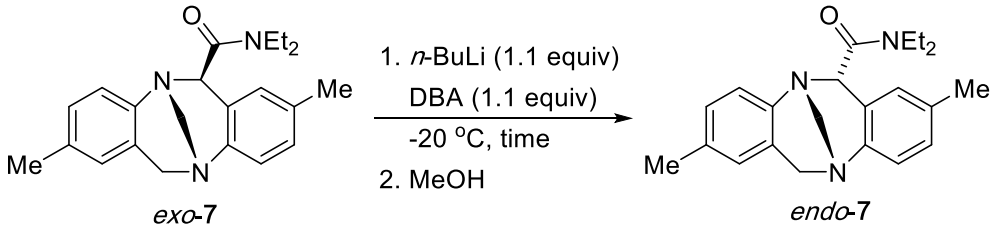

Entry	Time	*Endo*-**7**:*Exo*-**7** Ratio[a]
1	1 min	15:85
2	1 h	81:19
3	2 h	86:14
4	3 h	83:17
5	4 h	83:17
6	18 h	84:16

[a]Derived from ^{1}H NMR spectra of the worked-up reaction mixtures (see Experimental Section) by comparison with authentic pure materials. Reaction run until no change in composition of reaction mixture. *exo*-**7** and *endo*-**7** were the only products.

A preparative synthesis of *endo*-**8** was similarly carried out using the optimum conditions, as developed for the isomerization for *exo*-**7**, to afford the *endo*-**8** in 54% yield of isolated product in addition to recovered starting material, exo-**8** (25%) (Scheme 2). The structure of *endo*-**8** was confirmed by single crystal X-ray analysis (Figure 3).

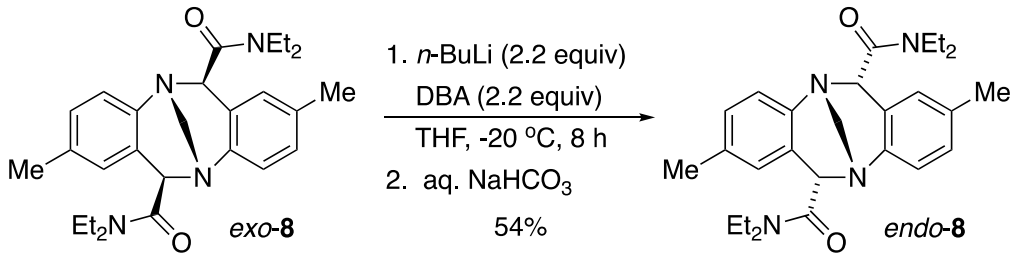

Scheme 2. Conversion of *exo*-**8** to *endo*-**8** under LiDBA conditions.

All of the preceding experiments involved quenching under kinetic conditions, i.e, the stereochemistry of the product is determined in the quenching of the intermediate enolate. We also wished to investigate the isomerization process under conditions of thermodynamic control. Thus, *exo*-**7** and *endo*-**7**, (see Table 5, entries 1 and 2) were separately treated with a catalytic amount of sodium methoxide (0.05 equiv) in methanol for a period of 2 weeks at room temperature. We observed that, under these conditions, *endo*-**7** underwent complete isomerization to *exo*-**7** (Table 5, entry 2). Conversely, *exo*-**7** did not undergo isomerization (Table 5, entry 1). Repeating the isomerization experiments of *exo*-**7** and *endo*-**7** in methanol-d_4, we observed the exchange of the C-6 α-proton in the both cases for deuterium (Table 5, entries 3 and 4).

These observations suggest that the isomerization of *endo*-**7** and *exo*-**7** takes place via a carbanion intermediate, most likely an aminoenolate, and that *exo*-**7** is the more stable of the two isomers.

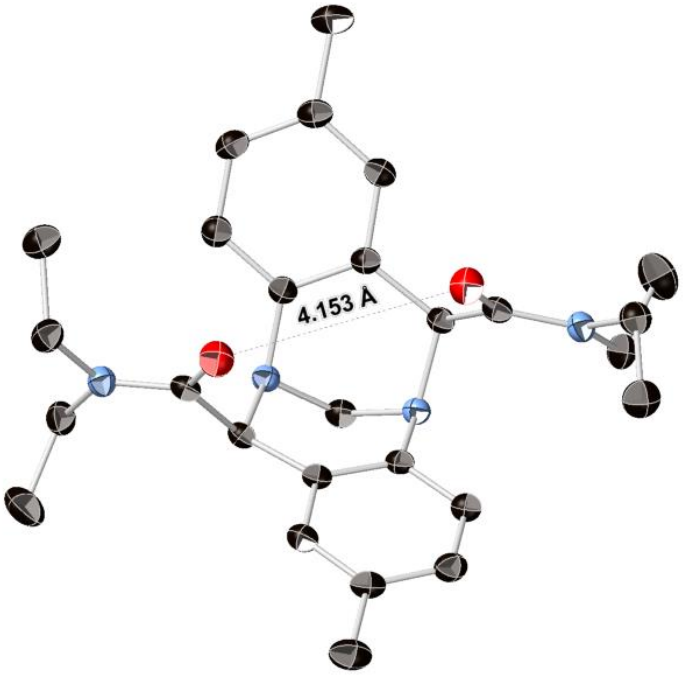

Figure 3. scXRD structure of *endo*-**8**. Thermal ellipsoids are shown at 30% probability. Hydrogen atoms are omitted for clarity. Black = carbon atom, blue = oxygen atom, red = nitrogen atom.

Table 5. Conversion of *endo*-**7** to *exo*-**7** using Thermodynamic Conditions. Enolization Process for Bases and Opening-Closing Process of the N-CH_2-N Bridge for Acids

Entry	Amide	Conditions	Product
1	*exo*-**7**	NaOMe (0.05 equiv), MeOH, rt, 2 weeks	*exo*-**7**
2	*endo*-**7**	NaOMe (0.05 equiv), MeOH, rt, 2 weeks	*exo*-**7**
3	*exo*-**7**	$NaOCD_3$ (0.05 equiv), CD_3OD, rt, 2 weeks	*exo*-**7**d_1
4	*endo*-**7**	$NaOCD_3$ (0.05 equiv), CD_3OD, rt, 2 weeks	*exo*-**7**d_1
5	*exo*-**7**	HCl (0.05 equiv), MeOH, rt, 24 h	*exo*-**7**
6	*endo*-**7**	HCl (0.05 equiv), MeOH, rt, 24 h	*exo*-**7**
7	*exo*-**7**	DCl (0.05 equiv), CD_3OD, rt, 24 h	*exo*-**7**
8	*endo*-**7**	DCl (0.05 equiv), CD_3OD, rt, 24 h	*exo*-**7**

As enantiomerically pure **1** is known to racemize under weakly acidic conditions,[35] treating either *exo*-**7** or *endo*-**7** with an acid should also result in isomer equilibration. This was indeed the case; treating both isomers independently with a catalytic amount of aqueous HCl resulted in the isolation of *exo*-**7** in both cases, indicating that this isomer is the more stable of the two. Performing the experiment in methanol-d_4 using a catalytic amount of DCl (Table 5, entries 7 and 8), showed no exchange of any hydrogens in *exo*-**7**. This is consistent with the isomerization mechanism involving opening of the methylene bridge to form an iminium ion,[35] and not an enolization mechanism and raises the interesting question of whether any enantiomerically pure TB derivative with an *exo* substituent placed at a benzylic methylene group would be stereochemically stable in acid. We are interested in examining this question.

In an effort to further evaluate the relative thermodynamic stability of the *exo* and *endo* isomers of **7**, Density Functional Theory (DFT) calculations at the M06/def2-TZVP level of theory were performed accounting for the THF solvent using the COSMO solvation model.[36-38] The amide was truncated to the corresponding dimethyl species (9) in order to simplify the calculations (Scheme 3).

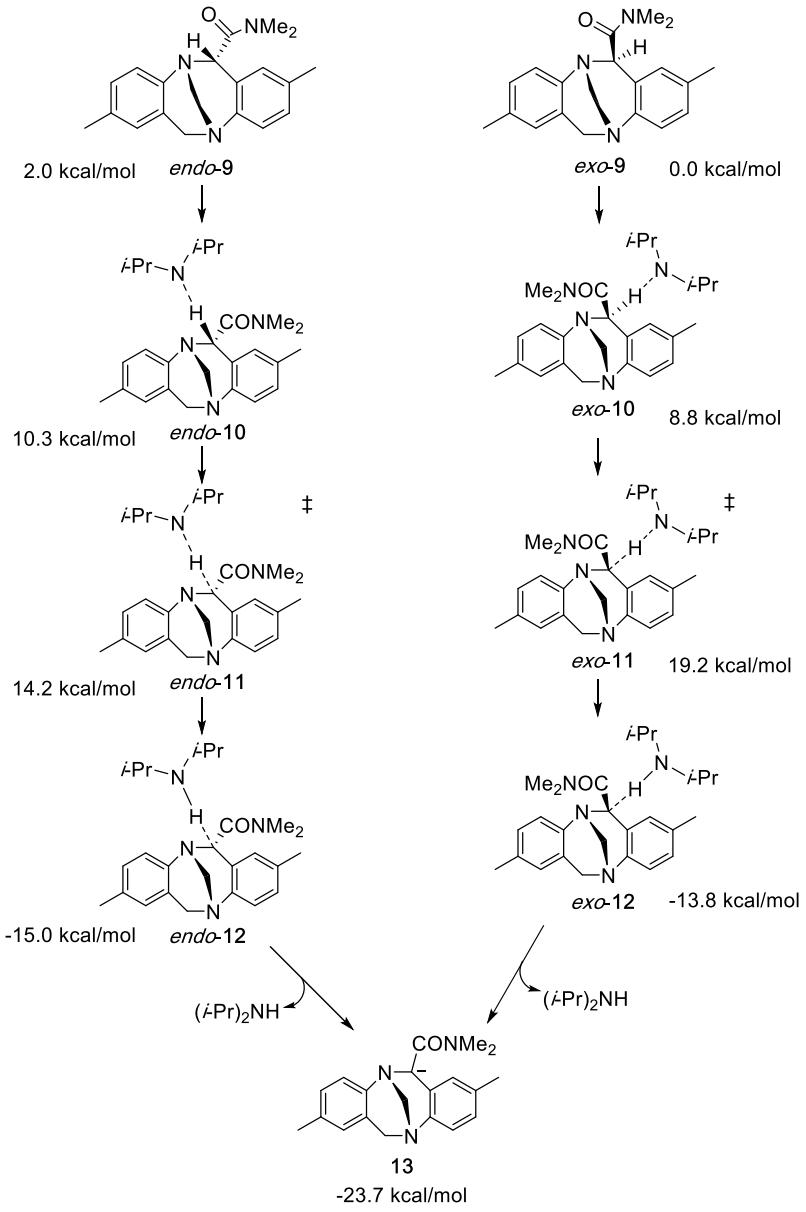

Scheme 3. *In silico* mechanism for the deprotonation of **9** and diisopropylamide.

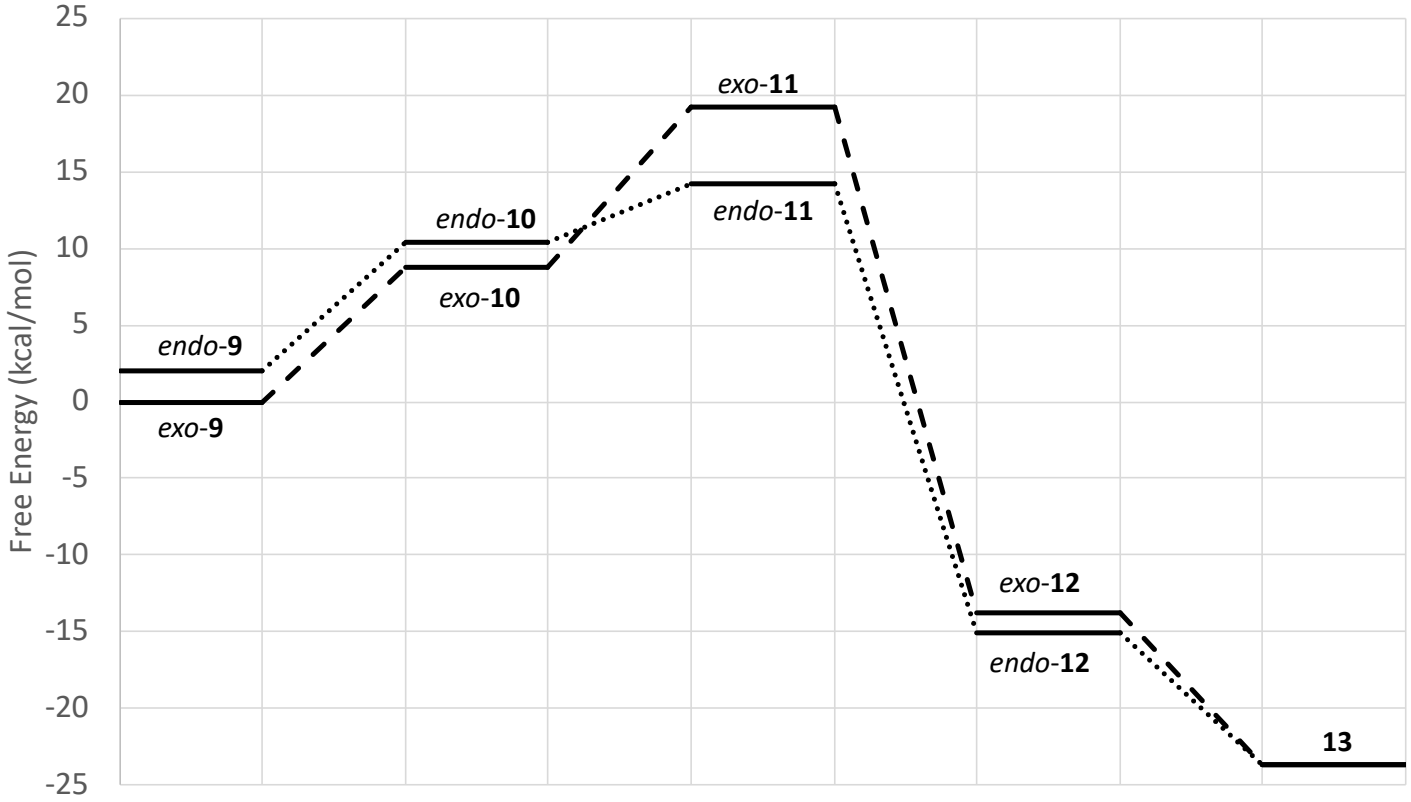

Figure 4. Free energy surface for the reaction mechanism outlined in Scheme 3.

The results showed *exo*-**9** to be 2.0 kcal/mol lower in energy than *endo*-**9**, supporting the idea that *exo*-**9** is the thermodynamically favored product. This is consistent with the experimental results obtained for both the acid and base-mediated equilibration of *exo*- and *endo*-**7** (Table 5).

In order to assist in rationalizing the results of *exo* to *endo* isomerization using kinetic bases, experimental findings were compared to a computational examination of the reaction mechanism for the isomerization using an experimentally relevant deprotonated DIPA reaction initiator. These calculations examined the energies for each isomer to undergo complexation with a DIPA anion in the absence of lithium cations, followed by a kinetically limiting proton transfer to form a stable enolate-DIPA complex, which can then dissociate in THF to produce the free enolate intermediate. Examination of the computational mechanism (Scheme 3, Figure 4) indicates that both stereoisomers undergo deprotonation by the diisopropylamide anion, with a thermodynamic driving force of more than 13 kcal/mol and a kinetic barrier less than 20 kcal/mol, suggesting relatively rapid formation of the enolate species, although deprotonation is expected to be slower for *exo*-**9** vis-à-vis *endo*-**9**, as deprotonation of the former results from removal of an *endo* hydrogen residing on the concave face of the molecule. Initial complex formation between **9** and the diispropylamide anion leads to a hydrogen-bonded complex **10**. This proceeds through transition state **11** to give an amide enolate complexed to diisopropylamine (**12**). Dissociation leads to the free enolate **13**.

Conversely, the quenching of the enolate intermediate in the presence of DIPA, may be treated as the protonation of the enolate complex by DIPA. Under these conditions, the thermodynamically favored *exo*-**9** product is predicted to form via a transition state that is 5.0 kcal/mol higher in energy than the TS for the *endo*-**9**. This elevated transition state energy appears to stem from the sterically hindered approach of the DIPA proton source on the *endo* face of the aminoenolate. Instead, the open *exo*-face should more easily

enable the approach of a proton source. Taken together, these computational results help confirm that quenching of the enolate should produce *exo*-**9** as a thermodynamically favored product, while *endo*-**9** will be kinetically favored (see Table S2, Supporting Information).

Conclusions

We have investigated the synthesis of *endo*-**7** and *endo*-**8** from their corresponding *exo* isomers (Figure 2). The reaction conditions were systematically optimized so that the maximum yield of the desired isomer was obtained. Furthermore, we established preparative routes to the *endo*-isomers from Tröger's base (**1**) (Scheme 4). This new approach to *endo*-substituted Tröger's base derivatives improves the overall yield over the previously reported method. The new method exhibits an overall yield of 60% for amide *endo*-**7** and 52% for amide *endo*-**8** over 2 steps as compared to 7% and 16% over 3 steps for the previous method, which was used to prepare esters **4** and **6**, respectively (Scheme 1).[8b] Finally, our study paves the way for the use of other functional groups as side chains that are able to induce enolization, to yield *endo* substituents on the Tröger's base skeleton. Further studies regarding the chemistry of *endo*-functionalized TB derivatives will be reported in due course.

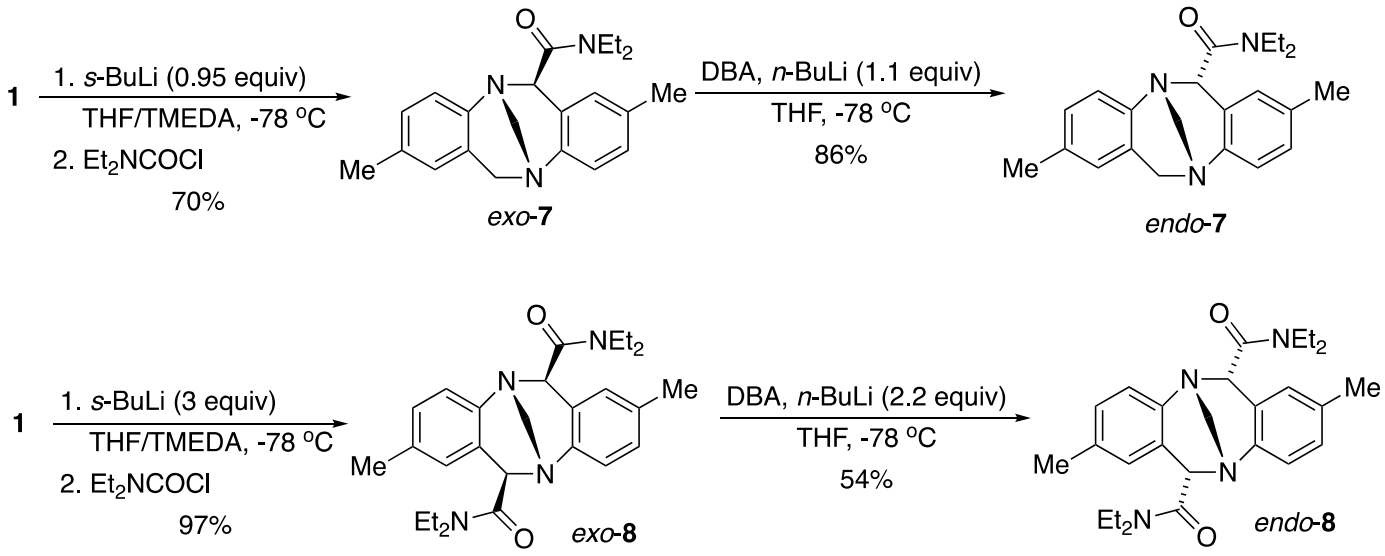

Scheme 4. Preparative routes to *endo*-**7** and *endo*-**8** from Tröger's base (**1**) based on the optimized conditions.

Experimental Section

General. *Exo*-**7** and *exo*-**8** were synthesized according to the protocol reported in our previous publication.[25] All chemicals were used as received from commercial sources without further purification. DIPA, DBA, TMEDA, DIPEA, DEA were dried with KOH pellets overnight and distilled under house vacuum prior to use. THF was dried with sodium and distilled under nitrogen. PE refers to petroleum ether (bp 40-60 °C). Precoated Merck silica gel 60 F_{254} plates were used for TLC analysis. Column chromatography was performed on silica gel (Davisil 35-70 µm). ^{1}H and ^{13}C NMR spectra were recorded on a 400 NMR spectrometer. Chemical shifts (δ) are reported relative to a shift-scale calibrated with residual NMR solvent peak $CDCl_3$ (7.26 ppm for

^{1}H NMR and 77.23 for ^{13}C NMR). Melting points were recorded on a Fischer-Jones apparatus, using plate technology. IR spectra were recorded on a FTIR spectrophotometer. HRMS were obtained on a Q-TOF microinstrument. Elemental analyses were performed by Mikroanalytisches Laboratorium KOLBE (Mülheim an der Ruhr, Germany).

Isomerization studies of *exo*-7 and *endo*-7

With MeOH/MeONa. *Exo*-**7** or *endo*-**7** (50.0 mg, 0.143 mmol) was dissolved in methanol (2 mL). Sodium (0.50 mg, 0.022 mmol) was added. The mixture was stirred for 24 h and neutralized by slow addition of HCl in methanol-d_4 (1.0 M). The solvent was removed *in vacuo,* the resulting residue was dissolved in $CDCl_3$, and a ^{1}H NMR spectrum was recorded on the resulting solution to determine the product ratio.

With CD_3OD/CD_3ONa. *Exo*-**7** or *endo*-**7** (50.0 mg, 0.143 mmol) was dissolved in methanol-d_4 (2 mL). Sodium (0.50 mg, 0.022 mmol) was added and the resultant mixture was stirred for 24 h. The mixture was made neutral by slow addition of DCl in methanol-d_4 (1.0 M). The solvent was removed *in vacuo,* the residue was dissolved in $CDCl_3$, and a ^{1}H-NMR spectrum was recorded of the resulting solution.

With HCl/MeOH/H_2O. *Exo*-**7** or *endo*-**7** (50.0 mg, 0.143 mmol) was dissolved in MeOH (5 mL). Aqueous HCl (1 M, 1 mL) was added and the mixture was stirred over 8-12 h at rt. The mixture was made alkaline (pH 10) by adding aqueous NaOH (1.0 M). Dichloromethane (5 mL) was added, the phases were separated, and the aqueous phase was extracted with additional dichloromethane (2×5 mL). The combined organic phases were collected and dried over Na_2SO_4, subjected to filtration, and the solvent was removed *in vacuo*. The residue was dissolved in $CDCl_3$ and the ^{1}H-NMR spectrum was recorded on the resulting solution.

With DCl/CD_3OD. *Exo*-**7** or *endo*-**7** (50.0 mg, 0.143 mmol) was dissolved in DCl in methanol-d_4 (1.0 M, 1 mL)). The mixture was stirred for 24 h and neutralized by slow addition of NaOMe in methanol-d_4 (1.0 M). The solvent was removed *in vacuo*. The residue was dissolved in methanol-d_4 and a ^{1}H NMR spectrum was recorded of the resulting solution.

Optimimized isomerization protocols for exo-7 and endo-7

Endo-**7** (0.050 g, 0.14 mmol), was dissolved in freshly distilled THF (2 mL) under N_2. Amine (1.1 equiv) was added and the solution was cooled to the desired temperature. A solution of *n*-BuLi (1.1 equiv) was added dropwise over 30 min. The reaction mixture was left for the required time and then quenched with the desired quenching medium. Water (5 mL) and dichloromethane (5 mL) were sequentially added and the phases separated. The aqueous phase was washed with additional dichloromethane (2×5 mL). The combined organic phases were washed with brine (5 mL) and dried (Na_2SO_4) and subjected to filtration. The solvent was removed *in vacuo* to dryness. The residue was dissolved in deuterated chloroform and a ^{1}H NMR spectrum was recorded of the resulting solution.

Preparative protocols for *endo*-7 and *endo*-8 based on the results from the optimization studies

***Endo*-2,8-dimethyl-6-(*N,N*-diethylcarbamoyl)-6*H*,12*H*-5,11-methanodibenzo[*b,f*][1,5]diazocine (*endo*-7[25]).** *Exo*-**7** (0.502 g, 1.44 mmol) was dissolved in dry THF (15 mL) under nitrogen. Dibenzylamine (0.31 mL, 1.6 mmol) was added under stirring and the mixture was then cooled to -20 °C. A solution of *n*-BuLi (2.5 M, 0.64 mL, 1.6 mmol) was added dropwise under vigorous stirring over 10 min. The solution was stirred at -20 °C for 2 h. The reaction mixture was quenched with 10 mL $NaHCO_3$ (aq, sat.). H_2O (20 mL) and CH_2Cl_2 (20 mL) were sequentially added and the phases were separated. The aqueous phase was extracted with an additional 3×25 mL CH_2Cl_2. The combined organic phases were washed with brine, dried (Na_2SO_4), subjected to filtration, and evaporated *in vacuo* to dryness. Purification by column chromatography (4×10 cm, PE-EtOAc 7:3) gave *endo*-**7**

(0.432 g, 1.24 mmol, 86% yield) as colorless crystals. R_f = 0.20 (PE:EtOAc 7:3); mp: 155-157 °C (Heptane/Diethyl Ether); IR (neat): 1641, 1489, 1428, 1375 cm^{-1}; ^1H NMR (400 MHz; $CDCl_3$): δ = 7.02 (d, *J* 8.1 Hz, 1H, H-10), 7.00 (dd, *J* 8.2, 1.9 Hz, 1H, H-9), 6.81 (dd, *J* 8.1, 1.4 Hz, 1H, H-3), 6.76 (brs, 1H, H-7), 6.72 (d, *J* 8.2 Hz, 1H, H-4), 6.70 (brs, 1H, H-1), 5.40 (s, 1H, H-6x), 4.64 (d, *J* 16.8 Hz, 1H, H-12x), 4.41 (dd, *J* 12.6, 1.5 Hz, 1H, H-13), 4.41-4.32 (m, 1H, N-C*H*$_2$-CH$_3$), 4.33 (d, *J* 12.6 Hz, 1H, H-13'), 4.19 (d, *J* 16.7 Hz, 1H, H-12n), 3.85-3.76 (m, 1H, N-C*H*$_2$-CH$_3$), 3.46 (dq, *J* 14.9, 7.3 Hz, 1H, N-C*H*$_2$-CH$_3$), 3.26 (dq, *J* 13.7, 6.9 Hz, 1H, N-C*H*$_2$-CH$_3$), 2.23 (s, 3H, Ar-C*H*$_3$), 2.18 (s, 3H, Ar-C*H*$_3$), 1.38 (t, *J* 7.2 Hz, 3H, -CH$_2$-C*H*$_3$), 1.29 (t, *J* 7.1 Hz, 3H, -CH$_2$-C*H*$_3$). ^{13}C NMR (100 MHz, $CDCl_3$): δ = 167.9, 145.8, 141.4, 134.6, 133.4, 129.5, 128.8, 128.4, 127.2, 127.1, 126.94, 126.91, 125.0, 68.5, 65.9, 58.7, 41.7, 40.7, 21.2, 21.0, 15.2, 12.6. HRMS-ESI$^+$: *m*/*z* $[M+Na]^+$ calcd for $C_{22}H_{27}N_3ONa$: 372.2099; found: 372.2052.

***Endo,endo*-2,8-dimethyl-6,12-di(*N,N*-diethylcarbamoyl)-6*H*,12*H*-5,11-methanodibenzo[*b,f*][1,5]diazocine (endo-8):** *Exo*-**8** (0.625 g, 1.39 mmol), was dissolved in THF (20 mL) and dibenzylamine (0.60 ml, 3.1 mmol) was added dropwise under stirring. The mixture was cooled to -78 °C. A solution of *n*-BuLi (2.5 M, 1.25 mL, 3.1 mmol) was added dropwise over 15 min. The mixture was allowed to warm to rt over 18 h. The reaction was quenched with 10 mL $NaHCO_3$ (aq, sat.). Additional H_2O (20 mL) and CH_2Cl_2 (20 mL) were added and the phases were separated. The aqueous phase was extracted with an additional 3×25 mL CH_2Cl_2. The combined organic phases were washed with brine, dried over Na_2SO_4, subjected to filtration, and evaporated *in vacuo* to dryness. Purification by column chromatography (5×10 1:1 PE:EtOAc) gave pure racemic *endo*-**8** (0.384 mg, 0.856 mmol, 54% yield) as colorless crystals. R_f = 0.1 (1:1 PE:EtOAc); mp: 230.1-231.0 °C (Heptane: EtOAc); IR (neat): 2974, 2930, 2871, 1633, 1487, 1430, 1215, 1136, 1059, 961, 816, 631, 557 cm^{-1}; ^1H NMR (400 MHz; $CDCl_3$): δ = 6.88-6.86 (d, *J* 7.8 Hz ,2H, H-3, H-9), 6.76-6.73 (m, 4H, H-1, H-4, H-7, H-H-10), 5.40 (s, 2H, H-6x, H-12x), 4.47 (s, 2H, H-13), 4.38-4.33 (m, 2H, N-C*H*$_2$-CH$_3$), 3.84-3.76 (m, 2H, N-C*H*$_2$-CH$_3$), 3.49-3.40 (m, 2H, N-C*H*$_2$-CH$_3$), 3.29-3.21 (m, 2H, N-C*H*$_2$-CH$_3$), 2.21 (s, 6H, Ar-C*H*$_3$), 1.39-1.35 (t, *J* 7.1 Hz, 6H, N-CH$_2$-C*H*$_3$), 1.30-1.26 (t, *J* 7.1 Hz, 6H, N-CH$_2$-C*H*$_3$). ^{13}C NMR (100 MHz; $CDCl_3$): δ = 167.5, 141.5, 134.2, 129.1, 128.2, 127.4, 126.6, 70.4, 66.3, 41.5, 40.5, 21.1, 15.1, 12.5. HRMS-ESI$^+$: *m*/*z* $[M+H]^+$ calcd for $C_{27}H_{37}N_4O_2$: 449.2917; found: 449.2914. Anal. Calcd for $C_{27}H_{36}N_4O_2$: C, 72.29%; H 8.09%; N, 12.49%. Found: C, 72.67%, H, 8.39%, N ,12.38%.

Acknowledgements

MH thanks the National Science Foundation, VS thanks NSERC Canada Discovery Grant Program, and KW thanks the Swedish Research Council for support. We thank Ms. Judy L. Snyder for assistance in proofreading the manuscript.

Supplementary Material

Proton and carbon-13 NMR spectra for *endo*-**7** and *endo*-**8**. X-ray crystallographic data for *endo*-**8**. Free energies for the calculated reaction mechanism. XYZ files for all structures in Scheme 3 were obtained by computational analysis.

References

1. Tröger, J. *J. Prakt. Chem.* **1887**, *36*, 225. https://onlinelibrary.wiley.com/doi/abs/10.1002/prac.18870360123
2. Yuan, C.; Li, J.; Xi, H.; Li, Y. *Mater. Lett.* **2019**, *236*, 9. https://www.sciencedirect.com/science/article/abs/pii/S0167577X18316227
3. Li, J.; Zhuge, X.; Yan, X.; Li, Y.; Yuan, C. *Opt. Mater.* **2019**, *90*, 257. https://www.sciencedirect.com/science/article/abs/pii/S0925346719301594
4. Yuan, C.-X.; Tao, X.-T.; Wang, L.; Yang, J.-X.; Jiang, M.-H. *J. Phys. Chem. C* **2009**, *113*, 6809. https://pubs.acs.org/doi/10.1021/jp8111167
5. Kammakakam, I.; Oharra, K. E.; Bara, J. E.; Jackson, E. M. *ACS Omega* **2019**, *4*, 3439. https://pubs.acs.org/doi/abs/10.1021/acsomega.8b03700
6. Fan, Y.; Li, C.; Zhang, X.; Yang, X.; Su, X.; Ye, H.; Li, N. *J. Membr. Sci.* **2019**, *573*, 359. https://www.sciencedirect.com/science/article/pii/S0376738818323299
7. Wang, Z.; Isfahani, A. P.; Wakimoto, K.; Shrestha, B. B.; Yamaguchi, D.; Ghalei, B.; Sivaniah, E. *ChemSusChem* **2018**, *11*, 2744. https://onlinelibrary.wiley.com/doi/10.1002/cssc.201801002
8. Dai, Z.; Tang, Y.; Sun, Q.; Liu, X.; Meng, X.; Deng, F.; Xiao, F.-S. *ChemCatChem* **2018**, *10*, 1900. https://onlinelibrary.wiley.com/doi/10.1002/cctc.201701534
9. Tao, L.; Niu, F.; Liu, J.; Wang, T.; Wang, Q. *RSC Adv.* **2016**, *6*, 94365. https://pubs.rsc.org/en/content/articlelanding/2016/ra/c6ra21196h#!divAbstract
10. Zhu, X.; Do-Thanh, C.-L.; Murdock, C. R.; Nelson, K. M.; Tian, C.; Brown, S.; Mahurin, S. M.; Jenkins, D. M.; Hu, J.; Zhao, B.; Liu, H.; Dai, S. *ACS Macro Lett.* **2013**, *2*, 660. https://pubs.rsc.org/en/content/articlelanding/2016/ra/c6ra21196h#!divAbstract
11. Del Regno, A.; Gonciaruk, A.; Leay, L.; Carta, M.; Croad, M.; Malpass-Evans, R.; McKeown, N. B.; Siperstein, F. R. *Ind. Eng. Chem. Res.* **2013**, *52*, 16939. https://pubs.acs.org/doi/10.1021/ie402846a
12. Kazem-Rostami, M. *New J. Chem.* **2019**, *43*, 7751. https://pubs.rsc.org/en/content/articlelanding/2019/nj/c9nj01372e/unauth#!divAbstract
13. Ling, X.; Wilcox, C. S. *Chem. Eur. J.* **2019**, *25*, 14010. https://onlinelibrary.wiley.com/doi/10.1002/chem.201901208
14. Hesselmann, A.; Ferraro, F. *J. Mol. Model.* **2019**, *25*, 1. https://link.springer.com/article/10.1007/s00894-019-3935-5
15. Bhayana, B.; Dickie, D. A. *Cryst. Growth Des.* **2018**, *18*, 6404. https://pubs.acs.org/doi/10.1021/acs.cgd.8b01138
16. Gardarsson, H.; Schweizer, W. B.; Trapp, N.; Diederich, F. *Chem. Eur. J.* **2014**, *20*, 4608. https://onlinelibrary.wiley.com/doi/10.1002/chem.201304810
17. Paliwal, S.; Geib, S.; Wilcox, C. S. *J. Am. Chem. Soc.* **1994**, *116*, 4497. https://pubs.acs.org/doi/10.1021/ja00089a057
18. Harmata, M.; Kahraman, M. *Tetrahedron: Asymmetry* **2000**, *11*, 2875. https://www.sciencedirect.com/science/article/abs/pii/S095741660000255X
19. Goldberg, Y.; Alper, H. *Tetrahedron Lett.* **1995**, *36*, 369 https://www.sciencedirect.com/science/article/pii/004040399402272D
20. Runarsson, O. V.; Artacho, J.; Wärnmark, K. *Eur. J. Org. Chem.* **2012**, *2012*, 7015.

https://onlinelibrary.wiley.com/doi/abs/10.1002/ejoc.201201249
21. Dolensky, B.; Elguero, J.; Kral, V.; Pardo, C.; Valik, M. *Adv. Heterocycl. Chem.* **2007**, *93*, 1. https://www.sciencedirect.com/science/article/pii/S0065272506930013
22. Valik, M.; Strongin, R. M.; Kral, V. *Supramol. Chem.* **2005**, *17*, 347. https://www.tandfonline.com/doi/abs/10.1080/10610270500073952
23. Demeunynck, M.; Tatibouet, A. *Prog. Heterocycl. Chem.* **1999**, *11*, 1. https://www.sciencedirect.com/science/article/pii/S0959638099800038
24. Dolensky, B.; Havlik, M.; Kral, V. *Chem. Soc. Rev.* **2012,** *41*, 3839. https://pubs.rsc.org/en/content/articlelanding/2012/cs/c2cs15307f/unauth#!divAbstract
25. Dawaigher, S.; Månsson, K.; Ascic, E.; Artacho, J.; Mårtensson, R.; Loganathan, N.; Wendt, O. F.; Harmata, M.; Snieckus, V.; Wärnmark, K. *J. Org. Chem.* **2015**, *80*, 12006. https://pubs.acs.org/doi/abs/10.1021/acs.joc.5b01921
26. Artacho, J.; Ascic, E.; Rantanen, T.; Wallentin, C.–J.; Dawaigher, S.; Bergquist, K. –E.; Harmata, M.; Snieckus, V.; Wärnmark, K. *Org. Lett.* **2012**, *14*, 4706. https://pubs.acs.org/doi/abs/10.1021/ol302022y
27. Artacho, J.; Wärnmark, K. *Synthesis* **2009**, 3120. https://www.thieme-connect.com/products/ejournals/abstract/10.1055/s-0029-1219617
28. Jensen, J.; Wärnmark, K. *Synthesis* **2001**, 1873. https://www.thieme-connect.com/products/ejournals/abstract/10.1055/s-2001-17525
29. Hansson, A.; Jensen, J.; Wendt, O. F.; Wärnmark, K. *Eur. J. Org. Chem.* **2003**, 3179. https://onlinelibrary.wiley.com/doi/abs/10.1002/ejoc.200300144
30. Jensen, J.; Strozyk, M.; Wärnmark, K. *J. Heterocycl. Chem*. **2003**, *40*, 373. https://onlinelibrary.wiley.com/doi/10.1002/jhet.5570400230
31. Artacho, J.; Ascic, E.; Rantanen, T.; Karlsson, J.; Wallentin, C.-J.; Wang, R.; Wendt, O. F.; Harmata, M.; Snieckus, V.; Wärnmark, K. *Chem. Eur. J.* **2012**, *18*, 1038. https://onlinelibrary.wiley.com/doi/10.1002/chem.201103228
32. Harmata, M.; Carter, K. W.; Jones, D. E.; Kahraman, M. *Tetrahedron Lett.* **1996**, *37.* 6267. https://www.sciencedirect.com/science/article/pii/0040403996013925
33. Harmata, M.; Rayanil, K.-O.; Barnes, C. L. *Supramol. Chem.* **2006**, *50,* 581. https://www.tandfonline.com/doi/full/10.1080/10610270600853477
34. Mehta, G.; Venkateswaran, R. V. *Tetrahedron* **2000**, *56*, 1399. https://www.sciencedirect.com/science/article/pii/S0040402099009217
35. Greenberg, A.; Molinero, N.; Lang, M. *J. Org. Chem.* **1984**, *49*, 1127. https://pubs.acs.org/doi/abs/10.1021/jo00180a035
36. Zhao, Y.; Truhlar, D. G. *Theor Chem Account* **2008**, *120*, 215. https://link.springer.com/article/10.1007/s00214-007-0310-x
37. Weigend, F.; Häser, M.; Patzelt, H.; R. Ahlrichs, R. *Chem. Phys. Lett.*, **1998**, *294*, 143. https://www.sciencedirect.com/science/article/pii/S0009261498008628
38. Eckert, F.; Klamt, A, *AIChE J.* **2002**, *48*, 369. https://aiche.onlinelibrary.wiley.com/doi/10.1002/aic.690480220